Ion Extraction from a Saddle Antenna RF Surface Plasma Source

V. Dudnikov[1,a)], R.P. Johnson[1], B. Han[2], S. Murray [2], T. Pennisi [2], C. Piller [2], M. Santana [2], M. Stockli [2], R. Welton [2], J. Breitschopf [3], G. Dudnikova[4,5]

[1]*Muons, Inc., Batavia, IL 60510, USA;* [2]*ORNL, Oak Ridge, TN 37831, USA;*
[3]*Taxes Lutheran University, Seguin, TX 78155,USA;* [4]*University of Maryland, College Park, MD- 32611-USA;*
[5]*Institute of Computational Technologies SBRAS, Novosibirsk, Russia*

[a)]Corresponding author: vadim@muonsinc.com

Abstract. Existing RF Surface Plasma Sources (SPS) for accelerators have specific efficiencies for H^+ and H^- ion generation around 3 to 5 mA/cm^2 per kW, where about 50 kW of RF power is typically needed for 50 mA beam current production. The Saddle Antenna (SA) SPS described here was developed to improve H^- ion production efficiency and SPS reliability and availability. At low RF power, the efficiency of positive ion generation in the plasma has been improved to 200 mA/cm^2 per kW of RF power at 13.56 MHz. Initial cesiation of the SPS was performed by heating cesium chromate cartridges by discharge as was done in the very first versions of the SPS. A small oven to decompose cesium compounds and alloys was developed and tested. After cesiation, the current of negative ions to the collector was increased from 1 mA to 10 mA with RF power ~1.5 kW in the plasma (6 mm diameter emission aperture) and up to 30 mA with ~4 kW RF power in the plasma and 250 Gauss longitudinal magnetic field. The ratio of electron current to negative ion current was improved from 30 to 2. Stable generation of H^- beam without intensity degradation was demonstrated in the AlN discharge chamber for a long time at high discharge power in an RF SPS with an external antenna. Continuous wave (CW) operation of the SA SPS has been tested on the small test stand. The general design of the CW SA SPS is based on the pulsed version. Some modifications were made to improve the cooling and cesiation stability. The extracted collector current can be increased significantly by optimizing the longitudinal magnetic field in the discharge chamber. CW operation with negative ion extraction was tested with RF power up to 1.8 kW from the generator (~1.2 kW in the plasma) with production up to Ic=7 mA. Long term operation was tested with 1.2 kW from the RF generator (~0.8 kW in the plasma) with production of Ic=5 mA, Iex ~15 mA (Uex=8 kV, Uc=14 kV).

INTRODUCTION

The development of a saddle antenna RF surface plasma source (SA RF SPS) was proposed to improve H^- ion production efficiency and SPS reliability and availability [1]. Improved plasma generation using a SA SPS was considered in [2-4]. Testing of H^- ion extraction at low RF power was presented in [5,6]. Existing RF SPSs for accelerators have specific efficiencies of H^+ and H^- ion generation ~ 3-5 mA/cm^{2}kW, where about 50 kW of RF power is typically needed for 50 mA beam current production from 7 mm emission aperture [7,8]. The high RF power required for the sources as well as triggering of the pulsed discharge can create problems for very long term operation. Extraction of positive and negative ions from the SA RF SPS at higher RF power and at duty factor up to 100% is considered in this work. The extracted collector current can be increased significantly by increasing the longitudinal magnetic field in the discharge chamber. At low RF power, the efficiency of positive ion generation in the plasma has been improved up to ~ 200 mA/cm^2 per kW of RF power at 13.56 MHz. Initial cesiation of the SPS was performed by heating the cesium chromate cartridges by discharge as was done in the very first versions of the

SPS [9,10]. A small oven to decompose cesium compounds and alloys [11,12] was developed and tested. After cesiation, the current of negative ions to the collector was increased from 1 mA to 10 mA with RF power ~1.5 kW in the plasma (6 mm diameter emission aperture) and up to 30 mA with ~4 kW RF power in the plasma and longitudinal magnetic field of ~ 250 Gauss. In tested version of SA RF SPS the specific efficiency of H^- production was increased up to ~ 20 mA/cm^2 kW. Stable generation of H^- beam without intensity degradation was demonstrated in the AlN discharge chamber for a long time with high RF power in RF SPS with external antenna.

The total efficiency of the surface plasma produced fraction of the H^- beam is a product of the probability of secondary emission of H^- caused by plasma bombardment of the collar surface around the emission aperture, the probability of extraction of emitted H^-, and the rate of bombarding plasma flux [10-15]. The coefficient of secondary emission of H^- is determined by surface properties (proper cesiation) and the spectrum of the plasma particles bombarding the collar surface around the emission aperture [12-15].

The cesiation was improved recently [7,8] and can be supported nearly optimal (deposition of carbon films and cesium intercalation (implantation) can be important for long time stable cesiation). The probability of extraction of H^- emitted from the collar surface is dependent on the surface collar shape [7-15], which was optimized recently to improve H^- emission. The problem of efficient plasma generation is being addressed by the development of new RF plasma generators with higher plasma generation efficiency and better concentration of useful plasma flux onto the internal surfaces of the collar around the emission aperture for lower RF power [1- 6]. In this design we use the saddle antenna, which has its RF magnetic field transverse to the source axis, combined with an axial DC magnetic field, to concentrate the plasma on the collar where the negative ions are formed by secondary emission [1- 6, 16].

Improving efficiency of H^- generation by solenoid magnetic field in SPS with the saddle antenna was demonstrated in [2,6] by production H^- beam with pulsed current up to 67 mA in the SNS test stand after the ELEBT.

SA SPS DESIGN

Figure 1 is the schematic of the large RF SA SPS, showing the AlN ceramic discharge chamber, saddle antenna, and DC solenoid. The chamber has an ID=68 mm. The saddle antenna with inductance L=3.5 μH is made from a water-cooled copper tube. The RF assisted triggering plasma gun (TPG) is attached to the discharge chamber on the left [4,7]. The extraction system is attached on the right side.

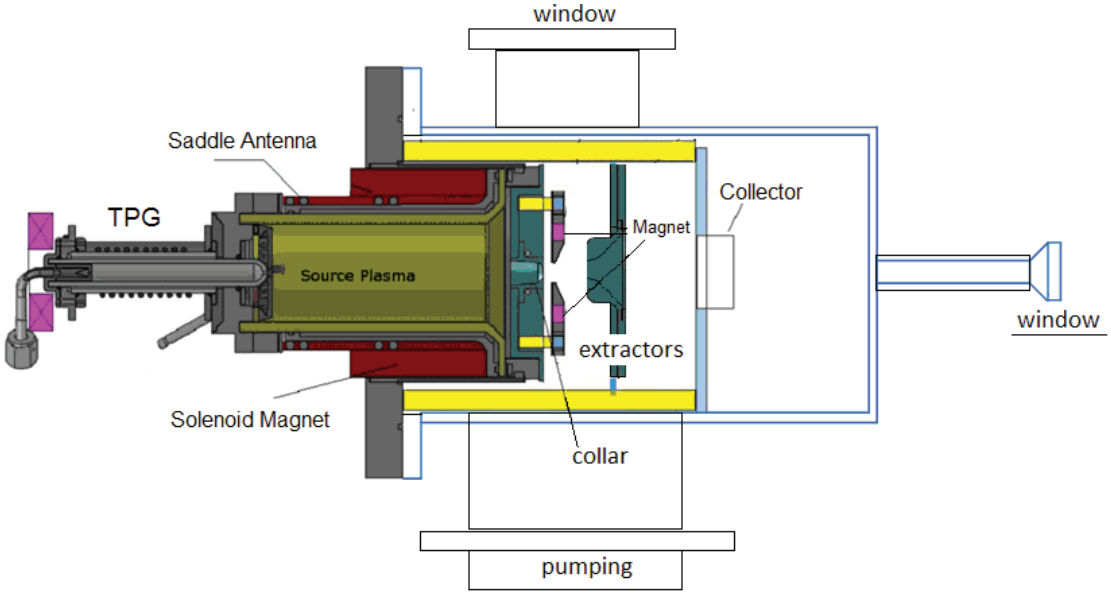

FIGURE 1. A schematic of the SA SPS with an extraction system, collector in vacuum chamber.

The plasma in the TPG is generated by a continuous wave (CW) RF discharge (13.56 MHz, ~250 W) and electrons are injected into main discharge chamber by the extraction voltage. The ion source is inserted into a

vacuum chamber pumped by a turbo molecular pump. The upper window is used for beam extraction observation. The front window (at right) is used to observe the back side of the collector while it is heated by ion beams.

The design of the SPS and the extraction system is shown in Fig. 2. The plasma flux, generated in the AlN discharge chamber (1) by the saddle antenna (2) is guided by the longitudinal magnetic field (created by solenoid (3)) to the a plasma electrode (4), with a conical collar (5) that defines the emission aperture. Ions are extracted from the cone by the extraction voltage Uex between the cone (5) and the extractor (7) and accelerated by the voltage across the second gap by voltage Uc on the accelerator electrode (10). Co-extracted electrons are well collected to the extractor (7) along magnetic field lines without drift in crossed ExB fields. The strong transverse magnetic field (up to 1 kG) is created inside the collar (5) by permanent magnets (8) inserted into the water cooled extractor (7) attached to the plasma electrode (4) through ceramic insulators. The transverse magnetic field before and after the extractor has opposite directions and the deflection of the extracted ions can be compensated. A PBGUNS simulation of H^- extraction is shown in Fig. 3.

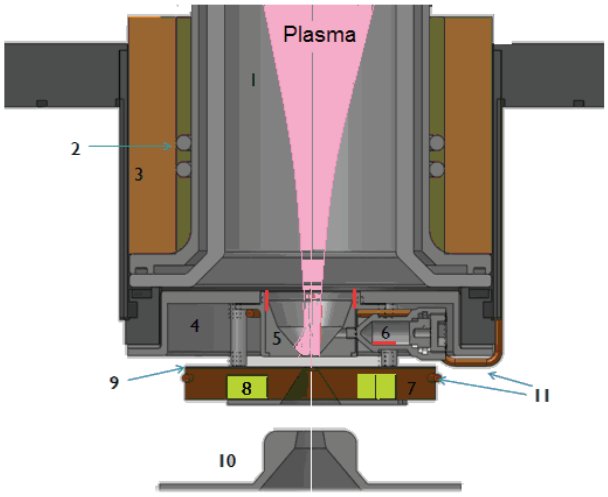

FIGURE 2. Design of SA SPS with extraction system. 1- AlN discharge chamber, 2- RF saddle antenna, 3- solenoid electromagnet, 4- plasma electrode (PE), 5- conical collar with emission aperture, 6- Cs oven, 7- extractor electrode, 8- permanent bar magnets, 9- molybdenum plate, 10- accelerating electrode, 11- water cooling lines.

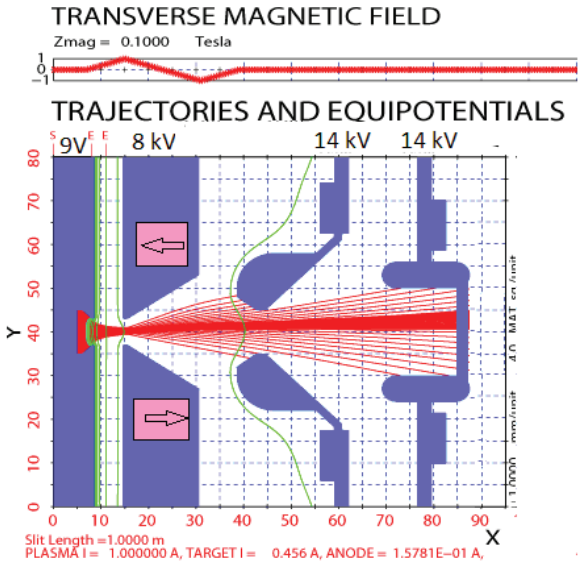

FIGURE 3. A schematic of ion beam extraction with simulation by PBGUNS (emission aperture is 6 mm). Transverse magnetic field distribution on top.

The transverse magnetic field distribution is shown in the top part of Fig. 3. The beam deflection by this magnetic field is almost compensated at extraction voltage (Uex=8 kV) and accelerating collector voltage Uc=14 kV (beam shifted up ~ 5 mm on the collector). At the normal accelerating voltage Uc=65 kV, this deflection and shifting is smaller and can be corrected by an Electrostatic Low Energy Beam Transport (ELEBT) adjustment. The strong transverse magnetic field Bt suppresses electrons escaping to the collector and the secondary emission is suppressed by magnets attached to the collector.

The superposition of solenoid longitudinal magnetic field Bs and transverse magnetic field Bt, with some ferromagnetic inserts, creates a complex magnetic configuration that determines the plasma flux distribution. Computer simulations of plasma electron trajectories in this field are shown in Fig. 4. The resulting magnetic field inside the conical collar can be perpendicular to the axis and is used for efficient suppression of electron diffusion through the emission aperture. The electron reflection by this magnetic mirror can support RF discharge at low gas density and low power. This resulting magnetic field compresses and bends the plasma flux as schematically shown in Fig. 2. The evidence of this plasma flux behavior is the trace of the dark film deposited on the conical collar surface shown in Fig. 5. With the increase of the solenoid current, this deposited area decreased up to the emission aperture. The SA SPS was tested with 6 mm diameter emission and extractor

apertures. The cesium vapor for the cone surface cesiation can be delivered to the emitter cone from Cs chromate cartridges inserted into the collar and heated by the plasma or from a resistive heated Cs oven (6).

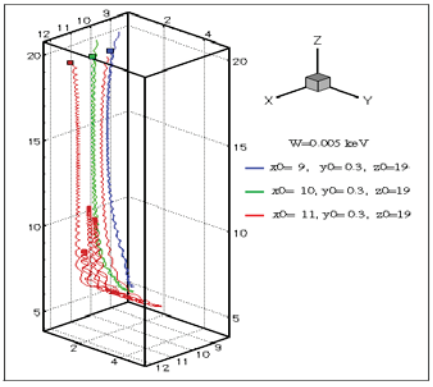

FIGURE 4. Examples of plasma electrons trajectories in magnetic field of SA SPS.

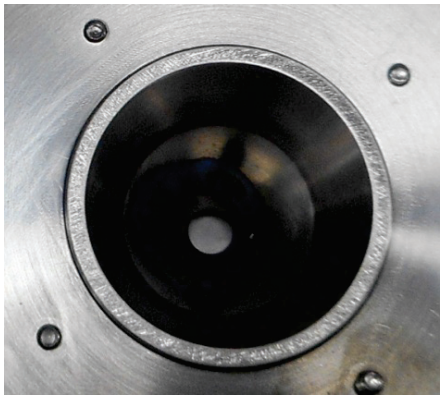

FIGURE 5. Internal surface of conical collar with autograph of plasma bombardment.

A photo of the assembled SA SPS with extraction/acceleration system and collector, collar cooling and plasma electrode with collar, Cs oven, ceramic insulators and cooling (right) is shown in Fig. 6.

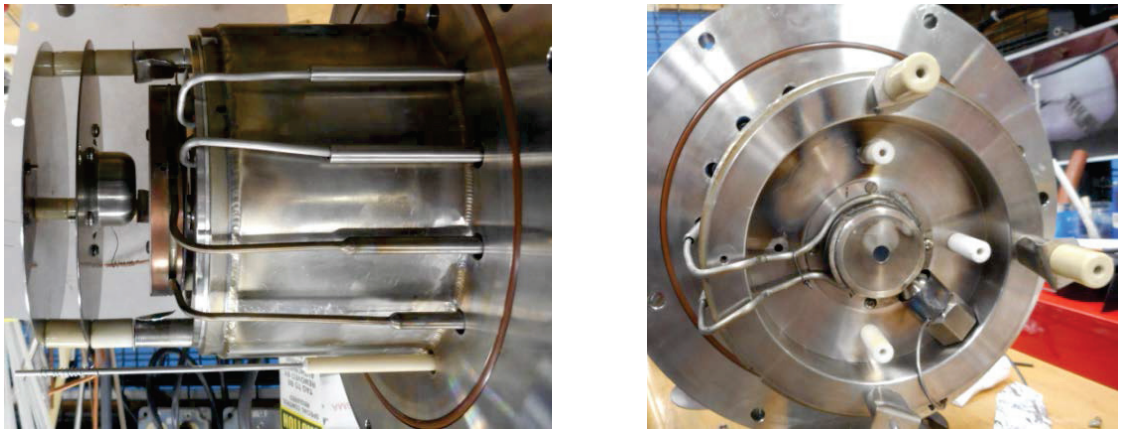

FIGURE 6. Assembled SA SPS with extraction system collector and extractor, collar cooling (left) and a front view of a plasma electrode with a collar, Cs oven, ceramic insulators and cooling (right).

EXPERIMENTAL RESULTS

The RF discharge in the TPG was excited by a 0.6 kW, 13.56 MHz RF generator. The SA discharge excitation used a compact Advanced Energy Industrial Apex 5513, 5.5 kW, 13.56 MHz RF generator. The RF power loss in the SA and matching network was ~1 kW, leaving up to ~4 kW to be used for plasma generation. The plasma electrode with Cs collar/cone was air cooled. The extractor, accelerator electrode, and collector were biased by high voltages Uex and Uc. Pulsed currents to these electrodes were registered by Pearson transformers with sensitivity 1 V/A.

A photo of the assembled SA SPS with extractor and collector is shown in Fig. 6. The magnetic field Bs up to 250 G was created by the solenoid with current Im up to 35 A and voltage Um up to 8 V.

The MKS mass flow controller was used for hydrogen gas injection with rate Q ~ 9 sccm to start the discharge. The pulsed discharge during TPG operation can be supported with Q ~ 4 sccm. The beam formation can be observed through the top window of the vacuum chamber.

Several versions of plasma generators with different antennas and magnetic field configurations were fabricated and tested in the small test stand. Pulsed RF (13.56 MHz) discharges with duration 1-2 ms, up to 60 Hz, and power up to ~1.5 kW in the plasma and 160 Hz, duty factor 5-25 % up to ~4 kW in the plasma were tested.

The measured positive ion emission current density distribution along the radius (registered by 7 small collectors on the plasma plate) was more peaked on the axis with increasing solenoid magnetic field [2, 3]. One diagnostic was the positive ion extraction through the 6 mm diameter emission aperture. A photo of the extraction system and collector during positive ion extraction is shown in Fig. 7. The ion beam extraction and collector heating by the ion beam on left side are visible on the photo. The plasma light from the emission aperture is visible on the right side. The collector is heated by the ion beam up to high temperature (~ >1000^{o}C).

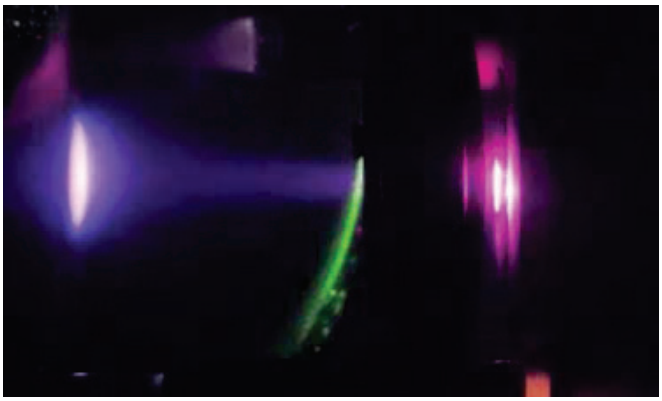

FIGURE 7. Photo of positive ion beam extraction and collector heating by the beam. Plasma light from emission aperture is visible at a right side. Collector is heated by ion beam up to high temperature (~ 1000^{o}C).

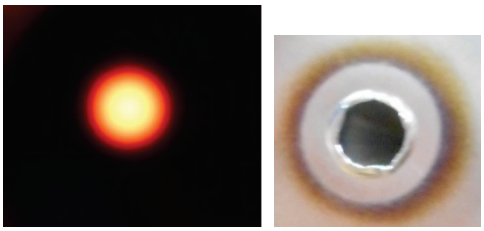

FIGURE 8. Photo of back side of tantalum collector heated by ion beam observed through a front window (left) and a collector melted by ion beam (right).A hole diameter is 6 mm.

The photo of the back side of the tantalum collector as observed through the front window, while heated by the positive ion beam, is shown in Fig. 8. The signal of the positive ion beam from the collector Ic=50 mA is shown in Fig. 9. The dependence of Ic on the extraction voltage Uex with RF power ~ 1.5 kW in the plasma is presented on Fig. 10. At low Uex, the ion beam diverges and hits the extractor with the emission of secondary electrons, leading to increased extraction current. Once Ux > 7 kV, the beam passes the extractor aperture without release of secondary electrons and Ic increases linearly with Ux.

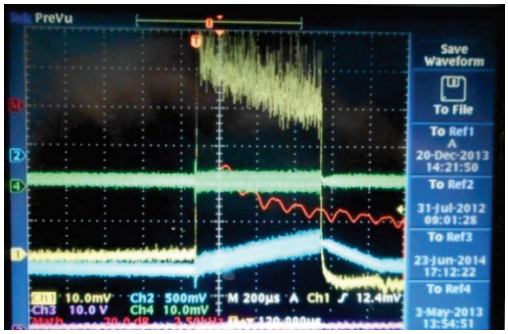

FIGURE 9. Signals of positive ion on collector - Ic =50 mA (Ch1; 10 mA/div) at RF power ~1.5 kW in the plasma and a signal of extraction voltage drop (Ch2; 5 kV/div). Time scale is 0.2 ms/div.

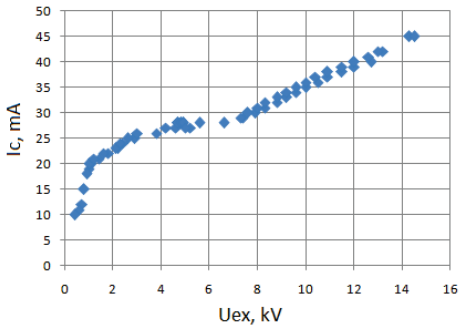

FIGURE 10. Positive ion collector current Ic vs extractor voltage Uex in pulsed mode.

The collector current Ic increases with increase of the solenoid field and also increases with decreasing of gas flow Q up to 4 sccm, necessary for stable discharge operation. The beam current noise increases with decreasing Q

and increase Bs. Up to 100 mA of positive ions can be extracted with 6 mm emission aperture at RF power ~ 2 kW in the plasma, and high solenoid field Bs~ 250 G.

The extraction of negative ions at low RF power (up to ~1.5 kW in the plasma) was tested before [5,6]. Before cesiation the pulsed collector current was Ic ~ 1 mA with extractor (electron) current up to Iex ~ 0.15 A. With increased RF power, up to 4 kW in the plasma, Ic was increased to ~ 3 mA and Iex to ~ 0.5 A. By cesiation at 1.5 kW Ic was increased up to 10 mA and Iex was decreased to 0.1 A. With increased RF power from the Apex 5513 RF generator to ~4 kW in the plasma, Ic was increased up to 30 mA.

A photo of negative ion extraction and collector heating by the negative ion beam is shown in Fig. 11. The plasma light from the emission aperture is visible on the right site and the extractor surface heating up to high temperature (up to yellow color) by co-extracted electrons is visible also. The collector is heated by the ion beam up to high temperature (~>1000°C). Ceramic insulator luminescence is excited by electron bombardment. In the right insert electrons are seen to drift in crossed ExB fields in the extraction gap. Tantalum collector heating by the negative ion beam is seen on the backside of the collector, shown in Fig. 12 together with trace of the beam bombardment. For Uex =8 kV extraction voltage and Uc=14 kV accelerating voltage, the position of the ion beam on the collector is shifted up by 5 mm, as predicted by the simulation shown in Fig. 3.

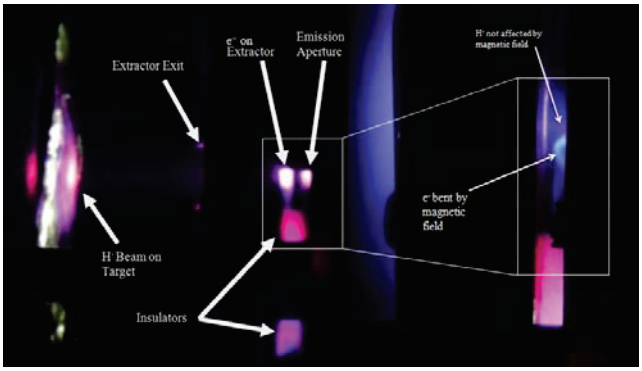

FIGURE 11. Photo of H^- beam extraction and collector heating by the beam. Light from emission aperture is visible at a right site and co-extracted electrons a heating the extractor surface up to high temperature (~ >1000°C). Collector is heated by ion beam up to high temperature (yellow color). Ceramic insulators luminescent are excited by electron bombardment.

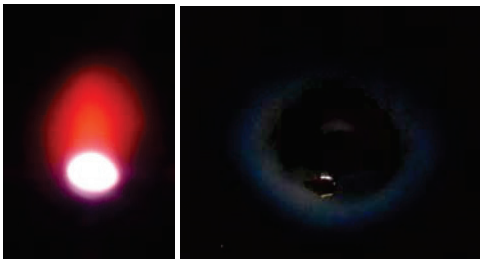

FIGURE 12. Back side of collector heated by negative ion beam. Bright spot is a plasma light visible through small hole (left), with an autograph of collector bombarding by negative ion beam (right; hole diameter is 2 mm).

Examples of collector signals Ic are shown in Figs. 13 and 14. After cesiation, the negative ion current to the collector Ic increased from 1 mA to 10 mA and the electron current to the extractor Iex reduced from 0.15 A to 0.1 A with RF power ~1.5 kW in the plasma. After "good" cesiation, Ic and Iex signals can have initial transient pulse values that are several times larger than the steady state values. With RF power ~4 kW in the plasma, Ic was increased up to 30 mA as shown in Fig. 14.

***

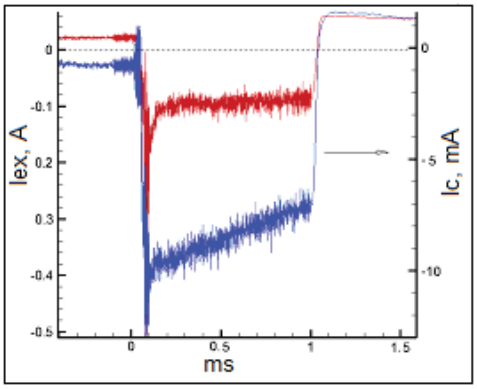

FIGURE 13. Signals from extractor (electron current, red) left scale and signal from collector Ic=10mA (negative ion current, blue) right scale. Signal slope is connected with a low inductance of the Pearson transformer.

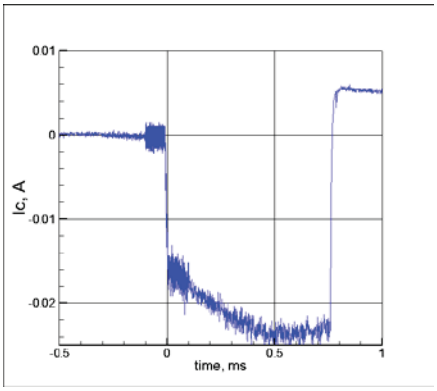

FIGURE 14. Signal from collector Ic=30mA (negative ion current). RF power is ~ 4 kW. Signal differentialization is connected with a low inductance of the Pearson transformer.

In the first tests of negative ion extraction, the ratio of co-extracted electron current to the beam current was relatively high after cesiation, Iex/Ic ~10. It was suspected that the increased electron current was due to the high RF frequency (13MHz, instead of 2 MHz in the SNS source). Fortunately, with improved cesiation and collar temperature optimization by compressed air cooling, Iex/Ic was decreased to 2. An example of a run with low Iex is shown in Fig. 15.

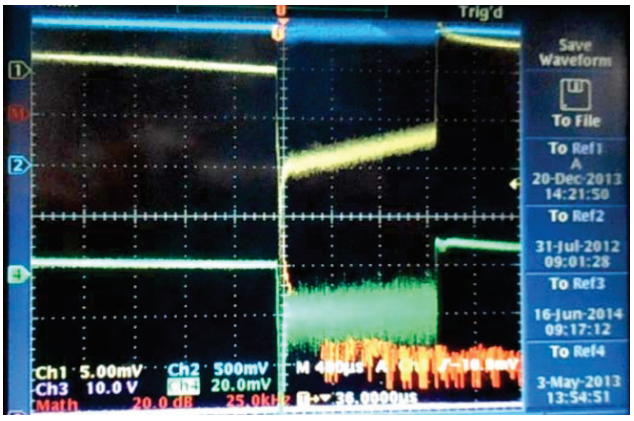

FIGURE 15. Signals from collector Ic=10mA (negative ion current, Ch1-5 mA/div) and a signal from extractor Iex=20 mA (electron current, Ch4-20 mA/div) Signal slope is connected with a low inductance of the Pearson transformer.

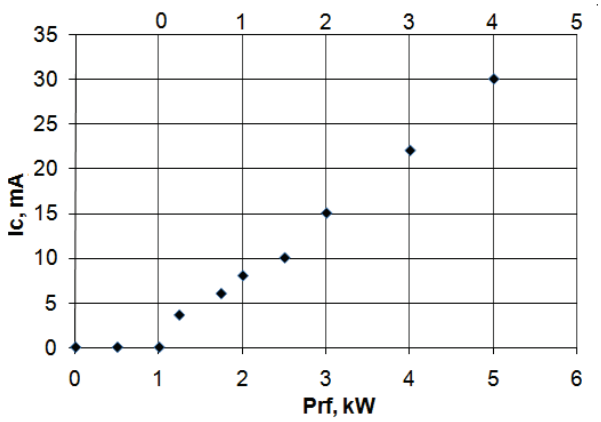

FIGURE 16. Dependence of the collector current Ic on RF generator power Prf (low scale) and RF power in the plasma (upper scale) with RF generator Apex 5513.

The dependence of Ic on RF power in the plasma Prf is shown in Fig. 16 (upper scale). The dependences of Ic on the solenoid voltage Um is shown in Fig. 17. The dependence of Ic on the extraction voltage is shown in Fig. 18. The collector current Ic increases by a factor of 7 as the longitudinal magnetic field Bl increases from 0 to 250 G and increases with the extraction voltage. The SA SPS operated with decreased gas flow down to Q~4 sccm (standard cm^3/minute), while the H^- current increased up to 10 mA at Prf=1.5 kW (the H^- generation efficiency was up to Ic/Prf = 6 mA/kW with cesiation). At low gas flow (Q~4 sccm) RF discharge is not supported with Um above 8.5 V. The longitudinal magnetic field from the solenoid at the emission aperture is below 50 G and does not affect the suppression and deflection of co-extracted electrons by the transverse magnetic field Bt~1 kG. The extraction current Iex has a significant level of noise with frequencies fn~1-2 MHz. The collector current Ic has an RF cross talk signal at 13.56 MHz .

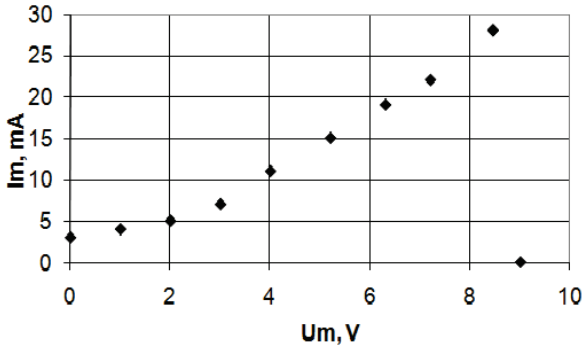

FIGURE 17. Dependence of the collector current Ic on a solenoid voltage Um.

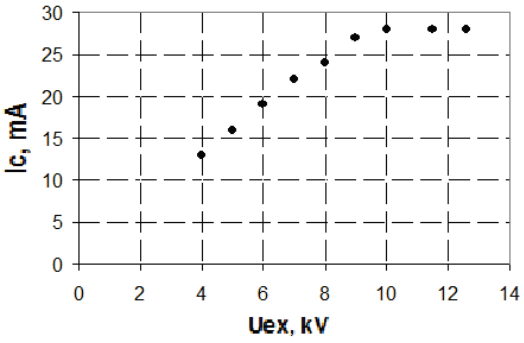

FIGURE 18. Dependence of the collector current Ic on an extraction voltage Uex.

CONTINUOUS WAVE OPERATION OF THE SA SPS

Continuous wave (CW) operation of the SA SPS has been tested in the small SNS test stand. The general design of the CW SA SPS is based on the pulsed version considered above [3, 4]. Some modifications were made to improve cooling and cesiation stability. The extracted collector current can be increased significantly by optimization of the longitudinal magnetic field in the discharge chamber. CW operation of the SA SPS with negative ion extraction was tested with RF power up to ~1.8 kW from generator (~ 1.2 kW in the plasma) with production up to Ic=7 mA. Long term operation was tested with 1.2 kW from the RF generator (~0.8 kW in the plasma and 0.4 kW is dissipated in the antenna and matching network) with production of Ic=5 mA, Iex ~15 mA (Uex=8 kV, Uc=14 kV). The initial cesiation of the SPS was performed by heating the cesium chromate cartridges by discharge and by further heating in an oven to decompose compounds and alloys. The behavior of the CW negative ion beam in the extractor and on the collector was similar to the pulsed beam behavior with the average intensities similar to those shown in Figs. 6 and 7. The collector was heated by the beam up to 1000°C. This is good evidence of negative ion beam extraction to the collector. The collector current decreases significantly and the extraction (electron) current increases when cesiation is not optimal.

The specific power efficiency of negative ion beam production in CW mode is up to Spe = 18 mA/cm^2 kW. (In the existing RF SPS the Spe ~ 2-3 mA/cm^2 kW [7,8]; in the TRUIMF filament arc discharge negative ion source [17,18] the best Spe is about 4 mA/cm^2 kW; in a compact Penning discharge SPS [12-15,19,20] the Spe is ~150 mA/cm^2 kW). During H^- beam extraction from an external antenna with RF discharges in the AlN discharge chamber, a slow degradation of H^- beam intensity after cesiation was observed [7]. It was suspected that this feature of AlN could not be eliminated. Fortunately, after some treatment of the AlN chamber and flanges, the continuous production of H^- beam with pulsed current ~ 50 mA (DF ~6%) was supported for ~30 days of operation [21]. The cooling of the AlN discharge chamber that was developed is able to remove the heat delivered by discharge with the average RF power up to 3 kW.

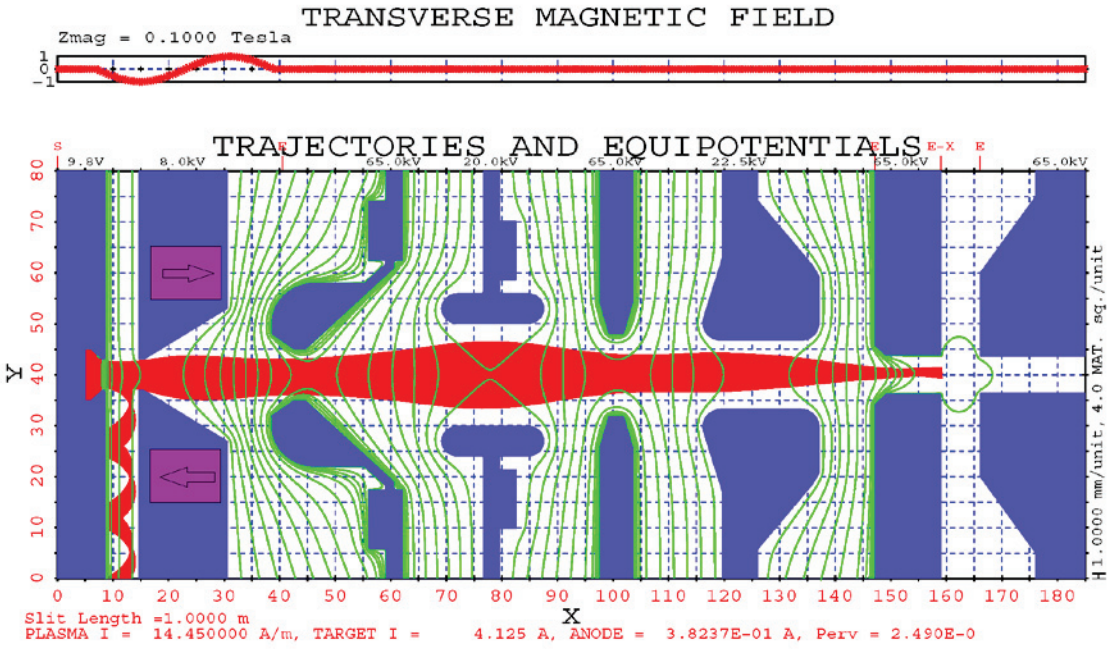

FIGURE 19. Simulation of high current beam extraction/transportation with ELEBT in SA RF SPS.

The simulation of high current beam extraction/transportation with an SA RF SPS with ELEBT is shown in Fig. 19, with extraction voltage Uex=8 kV, acceleration voltage Uc=65 kV, and lens voltage Ul=45 kV. The extracted ion current Ic is 40 mA. With an accelerating voltage Uc=65 kV the beam deflection and shifting is smaller and can

be corrected by electrostatic ELEBT adjustments. Electrons are drift in crossed ExB fields and are collected to the extractor along a magnetic field lines. This configuration of the SA RF SPS and ELEBT will be tested in the SNS Test Stand with H- beam transportation through electrostatic low energy transport (ELEBT).

ACKNOWLEDGEMENTS

The work was supported in part by US DOE Contract DE-AC05-00OR22725 and by STTR grant, DE-SC0002690 and DE-SC0011323.

REFERENCES

1. V. Dudnikov , G. Dudnikova and J. P. Farrell, "Surface Plasma Sources with Helicon Plasma Generators," in *AIP Conference Proceedings* ***925*** , 153 (2007).
2. V Dudnikov, et al., Rev. Sci. Instrum, **81**, 02A714 (2010).
3. V. Dudnikov, et al, Rev. Sci. Instrum. **83**, 02A712 (2012).
4. V. Dudnikov. et al., AIP Conference Proceedings 1390, 411, 2011.
5. V. Dudnikov, et al., AIP Conference Proceedings 1515, 456, 2013.
6. V. Dudnikov, et al., NAPAC 2013, http://accelconf.web.cern.ch/AccelConf/PAC2013/papers/tupsm22.pdf
7. R. F Welton., et al., Rev. Sci. Instrum**. 83**, 02A725 (2012).
8. M. P. Stockli, *Ion Injectors for High-Intensity Accelerators*, Reviews of Accelerator Science and Technology, Vol. 6 (2013) 197–219, World Scientific Publishing Company.
9. V Dudnikov, Method of Negative Ion Production, Patent cccp No. 411542, 10 March, 1972; http://www.findpatent.ru/patent/236/411542.html
10. Yu. Belchenko, G. Dimov and V. Dudnikov, Nuclear Fusion, **14**, 113 (1974).
11. V. Dudnikov, "Surface Plasma Source with Penning Geometry", in *Proceedings 4th All-Union Conference on Charged Part. Accelerators*, Moscow, V.1, p.323 (1974).
12. Y. I. Belchenko, G. I. Dimov, and V. G. Dudnikov, *Symposium on the Production and Neutralization of Negative Hydrogen Ions and Beams,Brookhaven, 1977,* BNL-50727 (BNL, Upton, NY, 1977), pp. 79–96.
13. Y. Belchenko and V. Dudnikov, "Surface negative ion production in ion sources," in *Production and Application of Light Negative Ions, 4th European Workshop*, edited by W. Graham (Belfast University, Belfast, 1991), pp. 47–66.
14. Yu. Belchenko, Rev. Sci. Instrum. **64**, 1385 (1993).
15. V. Dudnikov, Rev. Sci. Instrum. **63**, 2660 (1992).
16. V. Dudnikov et al., THPS026, in *Proceedings of IPAC2011*, San Sebastián, Spain, 2011; http://accelconf.web.cern.ch/AccelConf/IPAC2011/papers/thps026.pdf.
17. T. Kuo et al., Rev.Sci.Instrum. 67(3), 1314-1316, (1996).
18. T. Kuo, R. Baartman, L. Root, B. Milton, B. Uzat, D. Yuan, K. Jayamanna, M. McDonald, W. Z. Gelbart, N. R. Stevenson, P. Schmor and G. Dutto , "Injection study for high current H- cyclotrons," in *Proceedings of the 15th International Conference on Cyclotrons and their Applications*, Caen, France (1998).
19. Yu. Belchenko, A. Gorbovsky, A. Sanin, and V. Savkin, Rev. Sci. Instrum. **85**, 02B108 (2014).
20. V. Dudnikov, Rev. Sci. Instrum. **83**, 02A708 (2012).
21. R. F. Welton, V. G. Dudnikov, B. X. Han, S. N. Murray, T. R. Pennisi, M. Santana and M. P. Stockli, "Meeting the Future Needs of the SNS Facility using the External Antenna Ion Source and the Newly Constructed RFQ Test Stand ", *This Proceeding*.